Environmental Science and Pollution Research (2020) 27:10766–10777
https://doi.org/10.1007/s11356-019-07577-7

RESEARCH ARTICLE

# Phosphorus removal from wastewater by waste concrete: influence of P concentration and temperature on the product

Xiao Liu[1] · Huiyuan Zhong[1] · Yong Yang[1] · Linan Yuan[1] · Shibo Liu[1]

Received: 27 August 2019 / Accepted: 29 December 2019 / Published online: 16 January 2020


## Abstract

This study investigated the feature of phosphorus uptake by low-cost waste concrete. Adsorption isotherms, metal dissolution, influence of P concentration and temperature, as well as adsorbent regeneration were investigated. Chemical extraction, SEM, XRD, FTIR, and XPS were employed to determine the products of P sequestration. Results demonstrated that phosphate adsorption fitted the Langmuir isotherm model well, with estimated maximum phosphate adsorption capacity of 80.5 mg/g (10 °C). Of adsorbed phosphate, 72.1% could be desorbed when 0.1 M citrate buffer was used as eluant, and waste concrete could be recovered and reused for 4 times by the combination of eluting and roasting. Mechanisms including Ca/alkali dissolution, surface adsorption, and chemical precipitation are involved in the sequestration of phosphorus from wastewater by waste concrete. Weakly adsorptive phosphorus and Ca-P precipitate were the main products. P concentration was the major factor that affected P removal capacity and the product types, while temperature had certain effect at low P concentration. The dominant product was weakly adsorptive phosphorus for low P concentration at low temperature, which was substituted by Ca-P precipitate as temperature or P concentration increased. The increase of P concentration assisted both the increase of P removal potential and the formation of Ca-P precipitate to crystal DCPD.

**Keywords** P removal product · Concentration · Temperature · Waste concrete

## Introduction

Excess phosphate in water bodies can induce significant eutrophication and other environmental risk. Worldwide, phosphate pollution was largely attributed to the drainage from industrial, agricultural, and household sources. Therefore, phosphorus removal before wastewater discharge was considered as the most effective way to control phosphorus pollution. So far, the major techniques employed for phosphate removal included biological treatment, chemical precipitation, and medium adsorption, among which medium adsorption was an effective and low-cost process suitable for adverse condition (e.g., higher or ultra-low phosphate concentrations, unfavorable temperature).

Series studies were carried out recently to seek economical and sustainable adsorption medium for phosphate recovery. These adsorbents, including industrial solid waste (Chen et al. 2007; Park et al. 2016), construction refuse (Park et al. 2008), and clay adsorbents (Gimsing et al. 2007; Gan et al. 2009; Yue et al. 2010), generally contained metal elements such as Ca, Al, and Fe. Phosphate adsorption and precipitation occurred as P-containing sewage contacted with the materials. Among these adsorbents, Ca-rich materials such as flyash (Chen et al. 2007), steel slag (Park et al. 2016), and harden cement paste (Park et al. 2008; Wang et al. 2014; Yang et al. 2016) are low cost and easily obtainable, with good effect of P removal. It was concerned that $Ca^{2+}$ and $OH^{-}$ were released from the materials in wastewater to remove phosphorous by forming calcium phosphate. However, pollution risk such as heavy metal dissolution should be considered for flyash and steel slag as medium adsorbent (Feng et al. 2012; Stumbea 2013). In contrast, cement-based material can be cheap and sustainable with little environmental risk (Yang et al. 2016). Concrete contains plenty of cement gel, of which the potential

Responsible editor: Tito Roberto Cadaval Jr

**Electronic supplementary material** The online version of this article (https://doi.org/10.1007/s11356-019-07577-7) contains supplementary material, which is available to authorized users.

✉ Xiao Liu
xiaoliu200401@163.com

[1] College of Civil and Architectural Engineering, North China University of Science and Technology, Tangshan 063210, China

ability to improve water quality was confirmed even by concrete matrix (Luck et al. 2009). In China, waste concrete from urban construction exceeds $1 \times 10^9$ t annually (Zhou 2017), most of which were treated by landfill or even dumped illegally. Therefore, the utilization of waste concrete in phosphorus removal may bring an environmental value.

For cement-based material, precipitation (such as Ca-P and Al-P deposition) and surface adsorption were manifested to be the ways of phosphorus removal (Wang et al. 2014; Yang et al. 2016). Co-precipitation or competition was studied between phosphate and other negative ions (Park et al. 2008), and sorption isotherm and kinetics were fitted as well (Callery et al. 2016). In the previous research, higher P adsorption capacity was obtained at higher concentration, acidic pH, and higher temperature (Wang et al. 2014; Callery et al. 2016), and different crystalline phases were detected including $CaHPO_4 \cdot 2H_2O$, $AlPO_4$, tricalcium phosphate, and HAP (Forbes et al. 2004; Wang et al. 2014; Yang et al. 2016) to support the inferential mechanism. However, little research has focused on the product of phosphorus removal under different conditions. Considering that the material was both the seed of precipitate and the pool of metal ions and $OH^-$, heterogeneous nucleation and coprecipitation might coexist, and surface adsorption acted simultaneously driven by the surface charge (Forbes et al. 2004). Thus, the product feature would be related to the operating condition. It was confirmed for phosphorus removal by precipitation that pH and Ca/P molar ratio related to various Ca-P crystal products (Peng et al. 2018; Cichy et al. 2019), pH acted on surface adsorption by zeta potential (Peng et al. 2018), and temperature affected the crystallization process (Cichy et al. 2019). Nevertheless, temperature may influence the adsorption capacity of medium adsorption according to the exothermic/endothermic nature (Liu et al. 2011). Thus, the influence of pH, P concentration, and temperature on products should be concerned. It is notable that the liquid pH which acts on the surface charge (Liu et al. 2011) in medium adsorption process depends on both influnt pH and $OH^-$ released from the medium; thus, the equilibrium pH is more important than initial pH for the product analysis.

In the present study, the products of phosphorus removed by concrete was investigated at different P-concentration and temperature. P removal capacity under different conditions was discussed in terms of metal dissolving, equilibrium pH and $Ca^{2+}$ concentration. Chemical analysis, both quantitatively and qualitatively, was performed before and after P adsorption. The objectives of this study are (1) evaluate the P-adsorption capacity of waste concrete as adsorbents, (2) identify the effect of P concentration and temperature on the adsorption products, and (3) elucidate the mechanism of phosphorus removal.

## Materials and methods

### Preparation of waste concrete

Waste concrete was collected from local Civil Engineering Structural Laboratory, which was crushed and stacked as waste for years. The waste concrete was preliminarily crushed and screened to separate out sand and gravel of large particle size. Then, the sieve residue was crushed into powder < 0.1 mm in a grinder. And the powder was dried at 30 °C for 1 week.

### Metal dissolution from concrete

Metal ions reactive to phosphorus, including $Mg^{2+}$, $Al^{3+}$, $K^+$, $Ca^{2+}$, and $Fe^{3+}$, manifested their solubility from concrete through dissolution test. The test included phosphate series (50~1600 mg/L) and water series; the former was prepared by dissolving $KH_2PO_4$ in pure water, and the later was pure water with different pH value. To maintain the equilibrium pH closest to phosphate series, the initial pH of water series were adjusted by 0.1 M HCl with the same $H^+$ concentration to phosphate series. The experiments were carried out in a 20 °C, 200 rpm shaker with a series of capped 250-mL flasks, each containing 1 g of waste concrete and 100 mL of liquid, giving a solid: liquid ratio of 1:100. The batch experiments were executed in triplicates. After 24 h, samples were filtered through 0.45 μm Millipore paper and the concentration of above metal ions was observed.

### Phosphorus removal capacity of waste concrete

Phosphate series with initial P concentration from 0 to 1600 mg/L were tested their P-capturing potential under different temperature (10~40 °C), solid/liquid ratio and other conditions were in accordance with metal dissolution test. Directly after the end of the shaking period, equilibrium pH was measured. The suspensions were centrifuged at 4000 rpm and then filtered prior to analysis. The centrifugal residue was dried at 30 °C for 1 week for chemical and mineralogical investigations. And the filtrate was retained for $PO_4$-P and $Ca^{2+}$ analysis. P uptake amount was calculated by Eq. (1).

$$q_e = V(C_0 - C_e)/M \quad (1)$$

In the equation, $C_0$ and $C_e$ stand for the initial and equilibrium concentrations of P in the solution (mg/L), V represents the volume of solution (L), and M stands for the weight of the adsorbent (g).

To assess the adsorption isotherms process, relationship between $q_e$ and $C_e$ were fitted by Langmuir and Freundlich models as follows:

$$C_e/q_e = C_e/q_m + 1/(b \cdot q_m) \quad (2)$$

$$\ln q_e = (1/n)\ln C_e + \ln K_F \quad (3)$$

where $q_m$ is the maximum adsorption capacity corresponding to monolayer adsorption (mg/g), $b$ is the Langmuir adsorption constant (L/mg), $K_F$ is the Freundlich constant represents the relative adsorption capacity of the adsorbent (mg/g(L/mg)$^{-1/n}$), and $1/n$ is the heterogeneity factor denoting the adsorption intensity (Wang and Chen 2015; Wang et al. 2016, 2019).

### Chemical extraction of phosphorus

Sequential chemical extraction and analysis of inorganic phosphorus were conducted on P-containing residue according to the method described by T.R. Headley (Headley et al. 2003) to quantify the fractions of different P compounds in samples before and after reaction. Powder samples were extracted successively: (i) 1.00 g sample was extracted at room temperature for 16 h with 100 mL of 0.5 M $NaHCO_3$ with continuous agitation. This fraction stands for weakly bound P (W-P); (ii) the residue from (i) was added 100 mL of 0.1 M NaOH and stirred at room temperature for 16 h. The result represents Fe and Al associated P (Fe/Al-P); (iii) the residue from (ii) was leached at room temperature for 16 h with 100 mL of 1 M HCl with continuous agitation. The extraction substitutes for Ca/Mg associated P (Ca/Mg-P); (iv) the residue from (iii) was added 40 mL of 12 M HCl, and extracted in a water bath shaker at 80 °C for 20 min. After that, the sample was digested at room temperature for 1 h. This fration denotes P in very stable compounds (S-P).

All the extractions were performed in duplicate, and the extracts were centrifuged and filtered through 0.45 μm Millipore paper before analyzing. Simultaneously, concrete powder was extracted as control group.

### Characterization analysis for the products of P removal

Scanning electron microscopy (SEM) observation was conducted to examine the surface of samples with FEI Scios. The samples were coated with conductive platinum before SEM observations (Hitachi E-1010). Elemental concentration of both fresh and exhausted concrete was analyzed by X-ray fluorescence spectroscopy (XRF, PANalytical-Axios). Additionally, samples were examined mineralogy with X-ray diffraction (XRD, D/MaX2500PC, at 40 kV and 100 mA, Cu/kα). And further detection was performed with Fourier transform infrared spectroscopy (FTIR, Shimadzu IRAffinity-1s, KBr method) to seek P-containing functional group. XPS measurements were carried out on a high-resolution X-ray photoelectron spectrometer (Thermo ESCALAB 250xi USA) equipped with aluminum K radiation (1486.6 eV, 300 W). The binding energy of the C1s signal (284.6 eV) was used to correct the binding energy. Spectra of elements were fitted using a Shirley background and a Gaussian/Lorentzian (80/20) peak model.

Orthophosphate-P was analyzed by molybdenum blue method (SEPA China 2002), and mental ions were detected by ICP AES (Skyray Instrument, 2060T) and atomic absorption spectrophotometer (AAS, Persee TAS-990). All chemicals used were of analytical grade.

### Concrete recycle and reuse

Waste concrete was first saturated in 1600 mg/L phosphorus with the same operating conditions as 2.2 (including solid/liquid ratio, temperature, shaking speed, and parallel). After 24 h, the saturated samples were filtered for regeneration (desorption and roasting), and the filtrate was analyzed for phosphorus. For desorption, 0.1 M citrate buffer solution (pH 5) was used as eluant. After desorption, samples were adjusted to neutral and filtered, then calcinated at 900 °C for 0.5 h to recover the activity. As a contrast, saturated samples were roasted without desorption. The calcinated samples were then reused. For each saturating-regenerating cycle, P-adsorbed amount was calculated according to Eq. (1), and P-desorbed amount was calculated by Eq. (4).

$$q_d = V(C_e - C_0)/M \quad (4)$$

The meaning of $V$, $C_e$, $C_0$, and $M$ were the same to Eq. (1).

## Results and discussion

### Adsorption isotherm

Adsorption isotherms indicate the correlations between active sites of adsorbent and adsorbate concentration at equilibrium, which reveal the nature of adsorbate-adsorbent interaction (Wang et al. 2019). The fitting result of adsorption isotherms (Fig. 1 and Table 1) showed that both Langmuir and Freundlich models could describe the adsorption of phosphorus by concrete, and Langmuir model fitted the results better, meaning that monolayer adsorption was dominant. The maximum adsorption capacity calculated by Langmuir model ranged from 69.0 to 80.5 mg/g under the operating temperature. For Freundlich model, $0.1 < 1/n < 0.5$ is favorable for adsorption, and the obtained $1/n$ of waste concrete confirmed the appropriateness for phosphorus removal.

The maximum adsorption capacity ($q_m$) in Langmuir model is a useful parameter for adsorbent in scale-up considerations. Table 2 compared $q_m$ of concrete with other adsorbents (most of which came from solid waste). It can be seen that $q_m$ of waste concrete for phosphorus removal was relatively high,

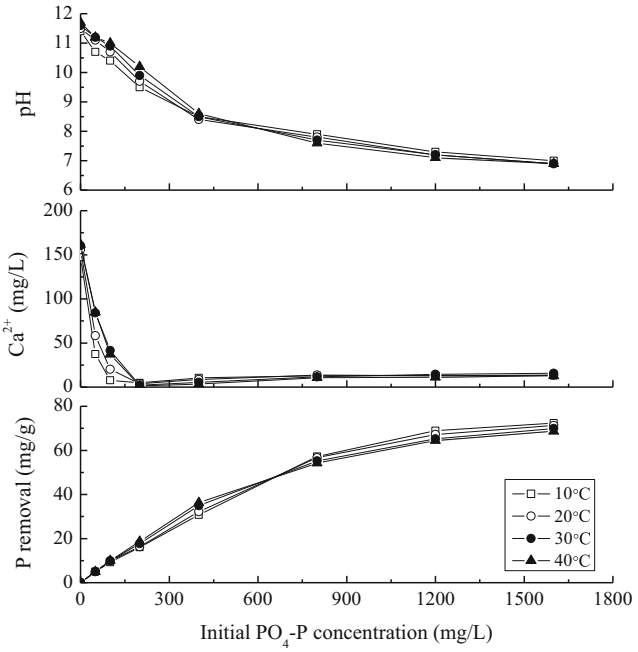


**Fig. 1** pH, $Ca^{2+}$, and P removal under different conditions

which suggested a better competitiveness of waste concrete in this field.

## Metal dissolution and phosphorus removal

Table 3 displays that Ca was overwhelming among the metal ions released from concrete to liquid at different pH. The dissociated Mg and K were much less than Ca and decreased with pH rise. The digestion of Fe and Al was neglectable. The less Ca, Mg, together with the eliminated K and P in P series, manifested that the depletion of these metal went along with phosphorus sequestration.

In Table 4, P and K were found to accumulate with the increase of P concentration, and Mg, Si, and Ca were the opposite trend. These gain or loss of component was relevant to concrete melting and insoluble salt deposition. Other element, such as Al and Fe, were observed to increase or decrease slightly, which was likely due to the relative concentration or dilution, since elements accumulation as well as components release were undergoing at the same time.

It is known that metal composition including Mg, Al, Ca, and Fe were typically reactive to phosphorus. Their dissociated ions were known to deposit phosphate in crystal or amorphous forms from liquid phase. And the oxides of Mg, Al, and Fe, as well as calcium carbonate were confirmed to facilitate the adsorption of P from aqueous solution (Shin et al. 2004; Antelo et al. 2010; Xu et al. 2014). Specially, K was proposed to included in the deposition of Struvite-type compounds $MgKPO_4{\cdot}6H_2O$ or $CaKPO_4{\cdot}nH_2O$ (Dickens and Brown 1972). $MgKPO_4{\cdot}6H_2O$ was confirmed to form in alkaline condition (Wilsenach et al. 2007; Xu et al. 2012), while $CaKPO_4{\cdot}nH_2O$ was considered unstable (Dickens and Brown 1972). Gao et al. (2018) suggested that $Ca^{2+}$ had adverse effect on $MgKPO_4{\cdot}6H_2O$ formation to form amorphous product.

According to Table 3, the amount of metal ion depleted by phosphate was $Ca^{2+} > K^+ \gg Mg^{2+}$ in our work, which showed the foremost role of calcium in phosphorus removal. Considering the massive expenditure of $K^+$ and its solubility in conventional solution, a hypothesis can be proposed that K was involved in Ca-P products. It seemed that the dosage of K, Ca, and P were not quantitative (the molar ratio of removed K/P rose from 0.28 to 0.62 as influent P increased from 50 to 1600 mg/L, while Ca available for P or K was irregular), which meant the unfixed composition of the product.

**Table 1** Fitting results of P to waste concrete by Langmuir model and Freundlich model

| Temperature (°C) | Langmuir model | | | Freundlich model | | |
|---|---|---|---|---|---|---|
| | $q_m$ (mg/g) | $b$ (L/mg) | $R^2$ | $1/n$ | $K_F$ | $R^2$ |
| 10 | 80.5 | 0.007 | 0.940 | 0.36 | 5.3 | 0.935 |
| 20 | 75.8 | 0.009 | 0.960 | 0.30 | 7.9 | 0.938 |
| 30 | 71.9 | 0.013 | 0.985 | 0.27 | 9.4 | 0.966 |
| 40 | 69.0 | 0.020 | 0.989 | 0.23 | 12.7 | 0.984 |

## Efluence of concentration and temperature on phosphorus removal by waste concrete

Figure 1 presents the influence of concentration and temperature on phosphorus removal by waste concrete. Overall, P removal capacity increased with the rise of initial concentration, and equilibrium pH exhibited the oppsite tendency. The residue $Ca^{2+}$ concentration first dropped and then recovered slightly as influnt P concentration increased from 0 to1600 mg/L, and the minimum $Ca^{2+}$ concentration appeared at 200 mg/L. From 10 to 40 °C, raising temperature had positive impact on P removal with elevated pH as $PO_4$-P was below 400 mg/L, but negative effect for higher concentration. P sequestration amount was 72.4 mg/g as initial $PO_4$-P was 1600 mg/L and temperature was 10 °C. In addition, an increasing trend of residue $Ca^{2+}$ was observed as temperature increased for low P samples.

The possible precipitation between phosphorous and concrete powder could be included by the following equations (Eqs. (5)~(10)):

$$H_2PO_4^- + OH^- \rightarrow HPO_4^{2-} + H_2O \quad (5)$$

$$H_2PO_4^- + 2OH^- \rightarrow PO_4^{3-} + 2H_2O \quad (6)$$

**Table 2** Comparison of waste concrete with other cheap adsorbents for maximum P-adsorption capacities

| Adsorbent | $q_m$ (mg/g) | Temperature (°C) | References |
|---|---|---|---|
| Fly ashes | 42.55 | Room temperature | Chen et al. (2007) |
| Red mud | 14.47 | 25 | Liang et al. (2012) |
| Attapulgite-based adsorbent | 42.0 | 25 | Yin and Kong (2014) |
| Steel slag | 3.2 | 25 | Park et al. (2016) |
| Cement paste | 62.1 | room temperature | Park et al. (2008) |
| Cement-based mortar | 30.96 | 25 | Wang et al. (2014) |
| Tablet developed from cement | 4.39 | 25 | Yang et al. (2013) |
| Waste concrete | 69.0–80.5 | 10–40 | Present study |

$$4Ca^{2+} + 2OH^- + 3HPO_4^{2-} \rightarrow Ca_4H(PO_4)_3 + 2H_2O \text{ (amorphous calcium phosphate, ACP)} \quad (7)$$

$$Ca^{2+} + HPO_4^{2-} + 2H_2O \rightarrow CaHPO_4 \cdot 2H_2O \text{ (DCPD)} \quad (8)$$

$$8Ca^{2+} + 4PO_4^{3-} + 2HPO_4^{2-} \rightarrow Ca_8H_2(PO_4)_6 \text{ (octacalcium phosphate, OCP)} \quad (9)$$

$$3Ca^{2+} + 2\ PO_4^{3-} \rightarrow Ca_3(PO_4)_2 \text{ (tricalcium phosphate, TCP)} \quad (10)$$

$$10Ca^{2+} + 6PO_4^{3-} + 2OH^- \rightarrow Ca_{10}(PO_4)_6(OH)_2 \text{ (hydroxyapatite, HAP)} \quad (11)$$

These reactions are influenced by factors such as pH, reaction time, etc. (Barca et al. 2013). Formation and transformation of metastable precursors may be observed depending on different conditions (Stumm and Morgan 1981). Typically, ACP was first-formed, which transformed subsequently into DCPD or OCP in acidic or neutral supersaturated solutions. There is precipitation or transformation of DCPD into OCP without involving ACP phase. The conversion of ACP to HA has been convinced via intermediate OCP or not at mean to high pH (Wang et al. 2014). Although HA is the most stable phase at pH above 4.0, intermediate phase may exist chronically since the formation of HA is much slower, and the conversion of ACP to more crystallized calcium phosphates may be time-consuming (Drizo et al. 2002; Wang et al. 2014).

In the case of phosphorus removal by concrete, pH and $Ca^{2+}$ were influenced by both the solubility of active ingredient and their depletion. The downtrend of equilibrium pH with influent $PO_4$-P confirmed the reaction an alkali-cost process. While the variation trend of $Ca^{2+}$ indicated the couple of sedimentary consumption together with solid dissolution, calcium consumption seemed to be limited by concrete dissolution. For samples with P less than 200 mg/L, ion diffusion was activated at higher temperature to strengthen the solubility of concrete (suggested by the higher pH and $Ca^{2+}$ concentration) to get better Ca-P precipitation. Such case encouraged apatite to flourish due to the higher pH (> 9.5). Nevertheless, calcium phosphate may be converted to acidic phases such as DCPD and OCP since pH dropped down at higher phosphorus concentration. This may bring smaller Ca/P molar ratio of calcium phosphate and less Ca consumption; thus, a small recovery of $Ca^{2+}$ in liquid emerged. Moreover, the sediment covered active sites at higher phosphorus strength to impede the further

**Table 3** Metal dissolving and phosphorus removal (mg/L)

| Equilibrium pH | | 11.1 | 10.7 | 9.7 | 8.4 | 7.8 | 7.2 | 6.9 |
|---|---|---|---|---|---|---|---|---|
| P series | P concentration | 50 | 100 | 200 | 400 | 800 | 1200 | 1600 |
| | Mg | 0.0 | 0.0 | 0.3 | 3.5 | 19.6 | 33.8 | 44.8 |
| | Al | 0.4 | 0.3 | 0.0 | 0.0 | 0.0 | 0.0 | 0.0 |
| | P removal* | 49.9 | 98.6 | 163.1 | 321.6 | 566.5 | 671.8 | 712.6 |
| | K removal* | 17.6 | 35.6 | 78.5 | 143.3 | 315.7 | 464.3 | 553.5 |
| | Ca | 58.2 | 20.2 | 3.8 | 8.5 | 13.5 | 12.9 | 13.5 |
| | Fe | 0.0 | 0.0 | 0.0 | 0.0 | 0.0 | 0.0 | 0.0 |
| Water series | Mg | 0.0 | 0.2 | 3.0 | 12.6 | 24.2 | 37.8 | 50.0 |
| | Al | 0.6 | 0.5 | 0.0 | 0.0 | 0.0 | 0.0 | 0.0 |
| | K | 9.4 | 9.7 | 13.7 | 17.8 | 19.2 | 19.9 | 21.5 |
| | Ca | 207.4 | 314.7 | 502.9 | 699.5 | 1017.6 | 1335.3 | 1441.2 |
| | Fe | 0.0 | 0.0 | 0.0 | 0.0 | 0.0 | 1.0 | 1.8 |

* P and K removal was calculated by the difference between raw water and equilibrium concentration

**Table 4** Elemental concentration in concrete before and after reaction at 20 °C (mass fraction, %)

| Sample | O | Mg | Al | Si | P | S | Cl | K | Ca | Ti | Fe |
|---|---|---|---|---|---|---|---|---|---|---|---|
| Fresh concrete | 35.86 | 5.25 | 3.54 | 12.6 | 0.00 | 1.05 | 0.08 | 0.65 | 28.17 | 0.39 | 3.49 |
| 400 mg/L | 37.31 | 4.59 | 3.23 | 11.22 | 4.49 | 0.34 | 0.03 | 0.93 | 26.07 | 0.38 | 3.21 |
| 800 mg/L | 37.18 | 2.82 | 2.99 | 9.39 | 7.39 | 0.25 | 0.03 | 1.08 | 25.66 | 0.34 | 2.67 |
| 1600 mg/L | 38.16 | 2.05 | 2.85 | 8.73 | 9.22 | 0.23 | 0.03 | 1.46 | 25.44 | 0.26 | 2.61 |

reaction (Yang et al. 2016). In this case, pH was much more influenced by the precipitation-solubility equilibrium of calcium phosphate rather than by the surplus $OH^-$ between emancipation and depletion. Therefore, the slightly degressive pH and P removal with temperature at high P concentration should be considered as the evidence of calcium phosphate ablation.

## Chemical extraction of phosphorus

As shown in Fig. 2 and Table 5, the major fractions of phosphorus extracted from used concrete were W-P and Ca/Mg-P, which summed to over 88% of the total phosphorus (TP). The two fractions increased with phosphorus concentration, bringing the growth of TP retention at different temperature. Fe/Al-P content was less than 0.5 mg/g in samples balanced by $PO_4$-P 200~800 mg/L, but increased to 3.2~6.7 mg/g in 1600 mg/L sample. Besides, the amount of S-P appeared to be negligible under any condition. As temperature rose from 10 to 40 °C, W-P diminished in low strength samples, but Ca/Mg-P displayed the opposite trend. Temperature effect on the proportion of the two parts was even significant for low strength samples, namely W-P and Ca/Mg-P in 100 mg/L samples occupied 71% and 29% respectively of TP at 10 °C, which changed to 49% and 51% respectively at 40 °C (data not shown).

W-P represented the phosphate bound to concrete through nonspecific adsorption (Headley et al. 2003). The adsorptive capacity of this part depended much on surface charge and competitive anions. It is known that pH has a predominant influence on surface charge, and higher pH derives more hydroxylated and electronegative surface to amplify the electric repulsion against phosphate. Therefore, the lower W-P of low phosphate samples and their descended with temperature should attribute to the higher residual pH, and the insignificant variation W-P of high strength samples ought to respond to their relatively stable pH at different temperature.

Ca/Mg-P involved both surface complexes and deposition on the solid-liquid interface, as well as Ca/Mg-P deposition from liquid (Headley et al. 2003). According to Table 3, the digestion and expenditure of Mg was far less than Ca for all

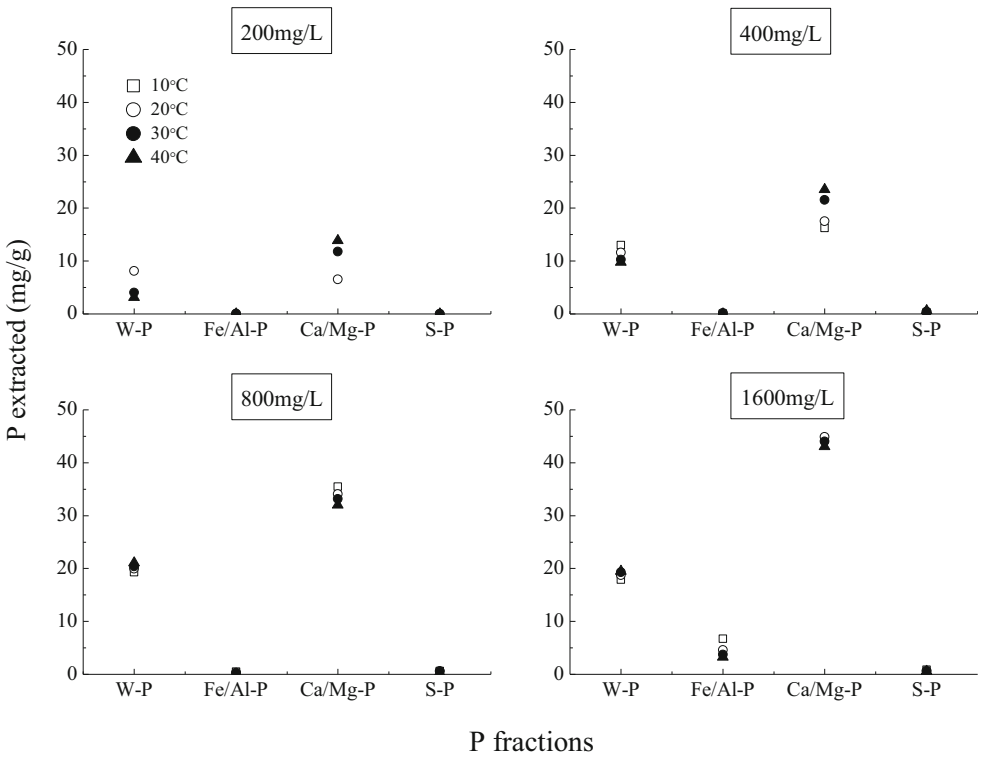


**Fig. 2** P extracted from concrete before and after reaction

**Table 5** The proportion of W-P and Ca/Mg-P in total phosphorus (%)

| Concentration (mg/L) | 200 | | | | 400 | | | | 1600 | | | |
|---|---|---|---|---|---|---|---|---|---|---|---|---|
| Temperature (°C) | 10 | 20 | 30 | 40 | 10 | 20 | 30 | 40 | 10 | 20 | 30 | 40 |
| W-P | 59 | 55 | 25 | 18 | 44 | 39 | 32 | 29 | 25 | 27 | 28 | 29 |
| Ca/Mg-P | 40 | 45 | 75 | 82 | 55 | 59 | 66 | 69 | 63 | 64 | 64 | 64 |

the samples; thus, the role of Mg on phosphorus recovery was insignificant. Consequently, the promotion of Ca/Mg-P by temperature at low P-concentration attributed to the elevated Ca-P reaction, while the shrinking Ca/Mg-P against temperature at high P-strength resulted from the dissolution of saturated Ca-P. On the other hand, temperature effect on surface coordination can be considerable in low strength samples. At pH above 9, the $PO_4^{3-}$ proportion increased in phosphate, and the endothermic coordination of Ca and P ($Ca^{2+}+PO_4^{3-}\leftrightarrow CaPO_4^-$) could be facilitated by temperature (Johansson and Gustafsson 2000).

The extractable Fe/Al-P fractions included both complexion and precipitation of phosphate to Fe/Al (Headley et al. 2003). The hardly release of Fe or Al from concrete (Table 3) suggested that seldom Fe/Al-P bouding occurred from precipitation reaction. Consequently, Fe/Al-P part in this research should be proposed as surface compounds of phosphate to Fe/Al oxides (hydroxides) existed at solid-liquid interface. For the interaction of Fe/Al oxide/hydroxide with phosphate, moderate to low pH was proved favorable related to surface protonation (Antelo et al. 2010; Stumm and Morgan 1981). Samples with alkaline equilibrium pH (< 800 mg/L) promoted the competition of $OH^-$ against phosphate to derive less Fe/Al-P formation. In contrast, the neutral equilibrium pH of 1600 mg/L samples was in favor of hydroxy-Fe/Al to bring about an increased Fe/Al-P value. Furthermore, temperature rise unbound surface complexion to decline Fe/Al-P portion for 1600 mg/L samples.

For low-strength samples, the greater part of W-P at low temperature meant that phosphorus was removed mainly by adsorption, the weakened adsorption and strengthened Ca/Mg-P fraction by temperature rise indicated the coexistence and competition between adsorption and precipitation. While the increased Ca/Mg-P proportion with P-concentration revealed that precipitation was promoted. It was proposed that higher P-concentration assisted phosphate to transport to the surface or inner of the adsorbent to enhance the interaction between phosphate and $Ca^{2+}$ (Yang et al. 2016). The precipitates continuously formed and grew off or on the adsorbent to consume more $Ca^{2+}$ and $OH^-$ as P concentration increased, which facilitated concrete dissolution to supply more $Ca^{2+}$ to bound phosphate, until saturation occured.

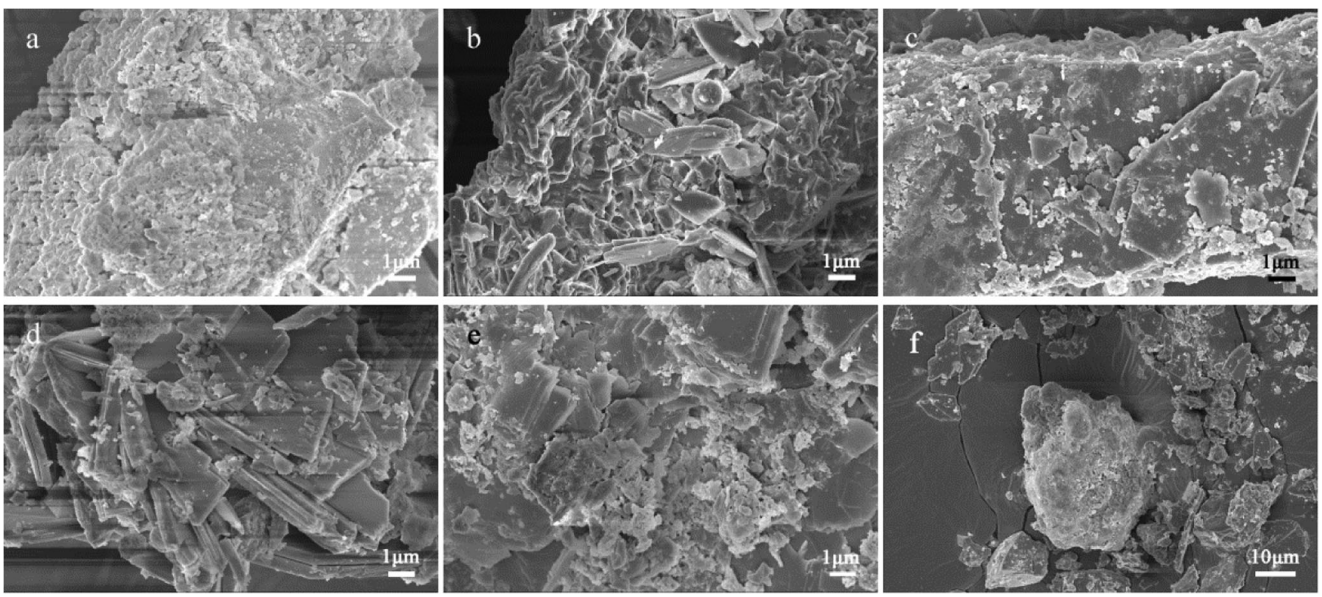


**Fig. 3** SEM of concrete powder before and after reaction. **a** Raw concrete; **b** 400 mg/L, 10 °C; **c** 400 mg/L, 40 °C; **d** 1600 mg/L, 10 °C; **e** 1600 mg/L, 40 °C; **f** 1600 mg/L, 40 °C

## Mineralogical and chemical characterization

Figure 3 manifests that samples from high P concentration were covered with flaky crystal, but those from low P concentration had less and irregular-shaped product. There were flaky product separated from concrete particles, especially in high P samples (Fig. 3f), which indicated that reaction occurred simultaneously at solid surface and liquid phase. Little difference was found between samples with same concentration regardless the temperature variation.

As shown in Fig. 4, the raw concrete contained such minerals as quartz ($SiO_2$), dolomite ($CaMg(CO_3)_2$) and calcite ($CaCO_3$). After reaction, brushite ($CaHPO_4{\cdot}2H_2O$, DCPD) was observed to emerge with enhanced intensity as P concentration increased. Additionally, calcite and dolomite were seen diminished with temperature respectively in 400 mg/L and1600 mg/L samples. For samples with the same concentration, little difference was found with temperature variation. No significant peak characteristic to crystalline phosphorus was detected in low strength samples (≤ 200 mg/L, data not shown).

In Fig. 5, the FTIR spectra of water (hydroxyl) and phosphorus displayed obvious difference between 400 and 1600 mg/L samples but little disparity between the same concentration at different temperature. The broad hydroxyl-peak of 400 mg/L sample (3442 $cm^{-1}$ and 1637 $cm^{-1}$, corresponded to $\nu_1$ and $\nu_2$ modes) attributed to the absorbed water, while the sharp peak of 1600 mg/L sample (3545 $cm^{-1}$/3552 $cm^{-1}$ and 1650 $cm^{-1}$) came from the coordinated water. The simultaneous appearance of $CO_3^{2-}$ (1438 $cm^{-1}$, 876 $cm^{-1}$, and 727 $cm^{-1}$, belong to $\nu_3$, $\nu_2$, and $\nu_4$ modes) and $PO_4^{3-}$ (1035 $cm^{-1}$ and 564 $cm^{-1}$/603 $cm^{-1}$, $\nu_3$ and $\nu_4$) in 400 mg/L samples coincided with the characteristic of $CO_3$-apatite (Comodi and Liu 2000; Yokota et al. 2006). The bands of $HPO_4^{2-}$ (1136 $cm^{-1}$ related to the stretching vibration of P=O, 1061 $cm^{-1}$, 986 $cm^{-1}$, and 528 $cm^{-1}$/576 $cm^{-1}$ associated with $\nu_3$, $\nu_1$, and $\nu_4$ modes of O-P-O) and P-OH (the dispersion peak located at 3163~3290 $cm^{-1}$), as well as the crystal water were in accord with DCPD in 1600 mg/L samples. In S1 (given in Supplementary information), the peaks of hydroxyl enhanced with phosphorus until coordinated water and DCPD emerged, proving that crystal product formed in higher phosphorus strength (this was consistent with XRD results).

The XRD and FTIR results supported the propose that DCPD tend to precipitate on the Ca-rich hydration materials in high phosphate strength and moderate to low pH (Forbes et al. 2004; Wang et al. 2014). Dicalcium phosphate (DCPD) was suggested the precursor of hydroxyapatite for a relatively short time. Although the transformation of dicalcium to hydroxyapatite could be several months (Forbes et al. 2004; Wang et al. 2014), the consisted of dicalcium and hydroxyapatite was reported after a few hours (Yang et al. 2016). This may related to equilibrium pH and the participation of $CO_3^{2-}$. $CO_3^{2-}$ participated in the precipitation of calcium phosphate in the atmosphere and competed for $Ca^{2+}$ with $PO_4^{3-}$. The participation of $CO_3^{2-}$ often resulted in poorly crystalline structures, especially at low phosphorus strength and pH below 10 (Yokota et al. 2006). The poorly crystalline needed long time to transformate into crystal hydroxyapatite. An increasing $PO_4^{3-}$ strength can produce the competitive superiority of it against $CO_3^{2-}$. And the substitution of $PO_4^{3-}$ for $CO_3^{2-}$ was described as ion exchange or dissolution-precipitation (Yoshimura et al. 2004). For the high P concentration samples in our experiment, the lower residual pH not only confirmed the domination of $PO_4^{3-}$ over $CO_3^{2-}$, but also induced $CaCO_3$ to dissolve, which followed by the sedimentation of dicalcium. Consequently, larger quantity of crystallinity (DCPD) was observed in these samples.

XPS was also a useful tool for analyzing the functional groups on surface of adsorbents. Functional groups could be semiquantitative analysis by detecting the local chemical state

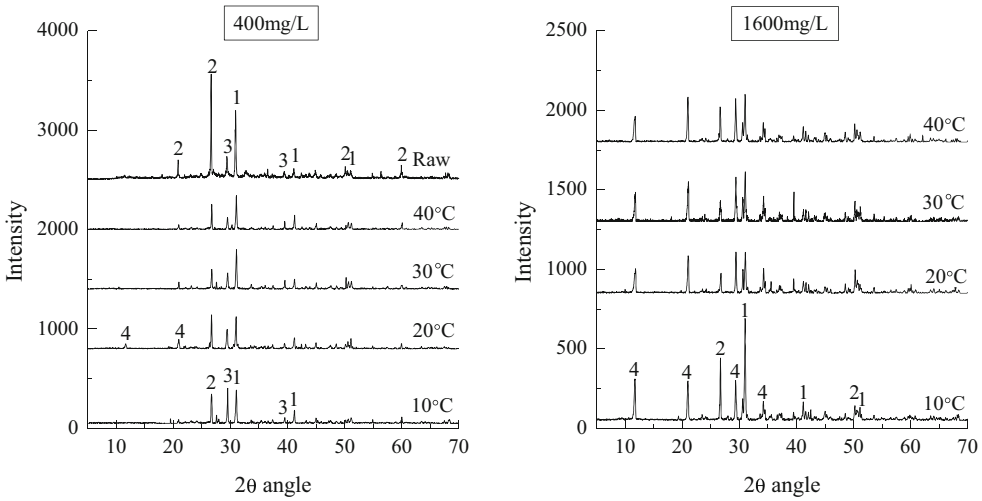


**Fig. 4** XRD analysis of concrete before and after reaction (1) $CaMg(CO_3)_2$, (2) $SiO_2$, (3) $CaCO_3$, (4) DCPD

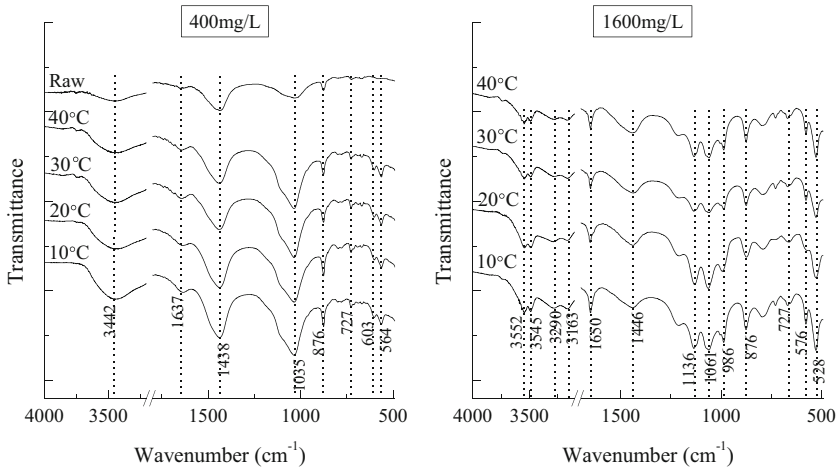


**Fig. 5** FTIR spectra of concrete before and after reaction

as well as binding energies change. In addition, this technique could allow for analysis of elements, such as oxygen, phosphorus, and other elements.

XPS spectra of the particles before and after phosphate sorption were evaluated in Fig. 6. It can be seen in the wide-scan spectra that new peaks of P (around 134 eV and 191 eV) emerged after phosphate sorption. This indicated that P was bound to functional sites on the surface of samples (Sleiman et al. 2016). The high-resolution spectrum of O 1s spectra before phosphate sorption can be deconvoluted into two overlapped peaks at 531.8 and 533.2 which were corresponding to C-O bonds ($CaCO_3$) and Si-O bonds ($SiO_2$), respectively (Moulder et al. 1992). After phosphate adsorption, the peak of C-O bonds replaced by P-O bonds at about 531.6 eV (Moulder et al. 1992). P 2p was divided into three peaks, 133 eV, 133.5 eV, and 134.2 eV, which corresponded to $PO_4^{3-}$ (non-crystal $CO_3$-apatite), $HPO_4^{2-}$ (DCPD) and amorphous P-O bonds to metal oxide, respectively (Yin and Kong 2014; Sleiman et al. 2016). The part of 133.5 eV and 134.2 eV increased in high concentration sample, meaning the increase of DCPD and adsorbed P, which was in accord with the results of chemical extraction and characterization. The molar ratio of $HPO_4^{2-}/PO_4^{3-}$ according to the peak areas obtained from the P 2p core level spectra was 1.32 and 2.41, respectively, to 400 mg/L and 1600 mg/L, confirmed the dominant position of DCPD in 1600 mg/L sample.

The above finding indicated that the mechanisms of phosphorus removal by concrete included the following process: (1) phosphorus adsorption to metal oxide/hydroxide, including surface complexation and electrostatic attraction; (2) phosphorus adsorption to carbonate through ion exchange or dissolution-precipitation; (3) Ca/alkaline release and Ca-P precipitation, including the precipitation on solid surface and bulk solution. The mechanism is illustrated in Fig. 7.

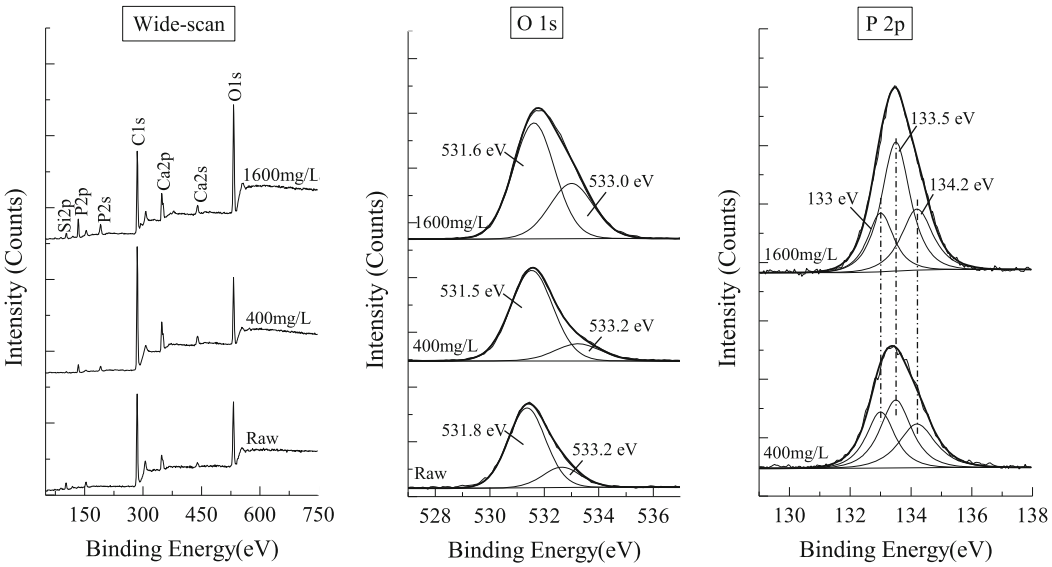


**Fig. 6** X-ray photoelectron spectroscopy of concrete before and after reaction at 10 °C

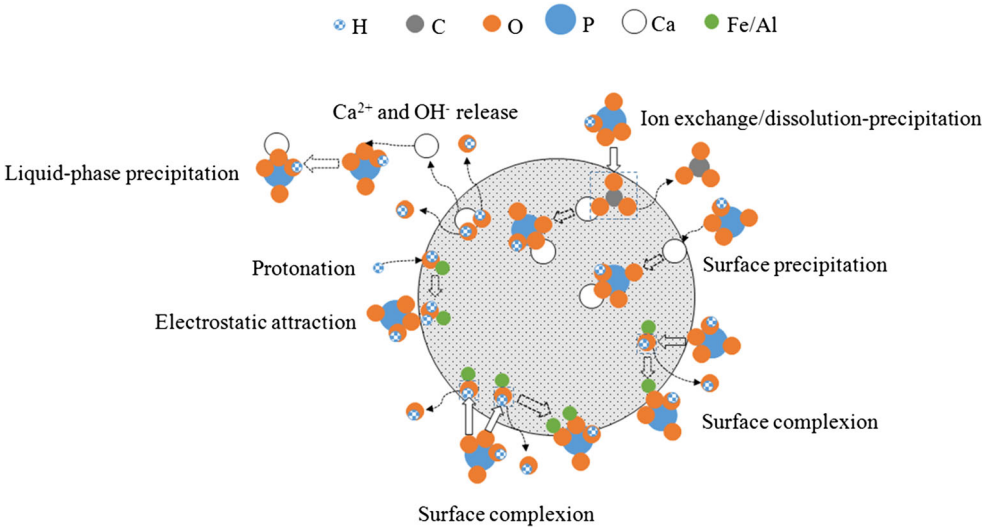


**Fig. 7** Illustration of the scheme mechanism of phosphorus uptake by concrete (dashed arrow: change into or move to, solidline arrow: substitute for)

## Concrete recycle and reuse

Figure 8 shows that the exhausted concrete could be cycle used after desorption and calcination. Totally about 72.1% of the adsorbed phosphate was recycled in 4 cycles when 0.1 M citrate buffer was used as eluent. The corresponding phosphates of adsorbed and desorbed were 185.17 mg/g and 133.56 mg/g, respectively. As mentioned above, phosphorus was bound to concrete by adsorption and Ca-P precipitation, whereas $H^+$ in desorption solution might destroy the combination. On the other hand, citrate ions might combine with the dissociated calcium instead of phosphate under neutral condition (Mitsionis et al. 2010). The formed calcium citrate was then decomposed into $CO_2$ and CaO during the following roasting. After regeneration, the active site of concrete was exposed so as to reuse for phosphorus removal. It is interesting that the exhausted concrete could be partially regenerated by calcinating directly. The adsorption capacity was recovered by roasting to 43.3% of the first use. However, the adsorption capacity tended to vanish after the second roasting. The recovery of P adsorption capacity after the first roasting might be related to the decomposition of $CaCO_3$ which was involved in the precipitate. As calcium was depleted by phosphorus in the further reuse cycle, losing of P adsorption capacity was observed.

## Implications for practical use

The results indicated that waste concrete could be sustainable and efficient adsorbent for phosphorus removal from aqueous. Compared with traditional phosphate precipitation, waste concrete was cheap and available as the amount of building waste was considerable in the present world. Besides, the application of waste concrete for phosphorus removal provided a way of

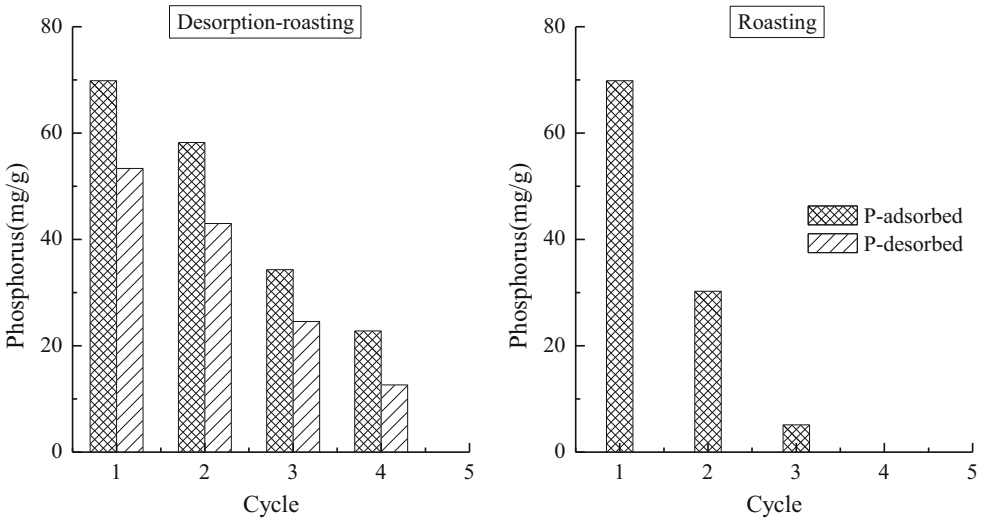


**Fig. 8** Concrete recovery and phosphorus recycling

high-value reuse for building waste. Thus, the application of waste concrete for phosphorus removal was economic and environmental protection. What is more, using waste concrete as phosphorus adsorbent/precipitant can be convenient in wastewater treatment process. The reaction of the method was fast and the product was easy settlement, thus common equipments or structures can be used for stirring and settling.

## Conclusion

Waste concrete exhibited excellent P adsorption ability. The process of P adsorption matched Langmuir isotherm model well. The estimated maximum phosphate adsorption capacity was 80.5 mg/g (10 °C), better than many adsorbents from solid waste. The removal of phosphorus by waste concrete is a simultaneous process of Ca/alkali dissolution, surface adsorption and chemical precipitation, weakly adsorptive phosphorus and Ca-P precipitate were the main products. Concentration was the major factor that affected P uptake capacity and the product types, while temperature had certain effect at low P concentration. The dominant product was weakly adsorptive phosphorus for low P concentration at low temperature, which was substituted by Ca-P precipitate as temperature or P concentration increased. The increase of P concentration assisted both the increase of P removal potential and the precipitation of Ca-P into crystal DCPD. The P-saturated concrete could be regenerated by the combination method of citrate eluting and roasting, which helped the concrete recover and reuse for 4 times.

**Funding information** This study is supported by the Science and Technology Planning Project of Hebei Province (No. 17273802D) and Higher Educational Science and Technology Program of Hebei Province (No. QN2015075).

## References

Antelo J, Fiol S, Pérez C, Mariño S, Arce F, Gondar D, López R (2010) Analysis of phosphate adsorption onto ferrihydrite using the cd-music model. J Colloid Interface Sci 347:112–119

Barca C, Troesch S, Meyer D, Drissen P, Andres Y, Chazarenc F (2013) Steel slag filters to upgrade phosphorus removal in constructed wetlands: two years of field experiments. Environ Sci Technol 47:549–556

Callery O, Healy MG, Rognard F, Barthelemy L, Brennan RB (2016) Evaluating thelong-term performance of low-cost adsorbents using small-scale adsorption column experiments. Water Res 101:429–440

Chen JG, Kong HN, Wu DY, Chen XC, Zhang DL, Sun ZH (2007) Phosphate immobilization from aqueous solution by fly ashes in relation to their composition. J Hazard Mater 139:293–300

Cichy B, Kużdżał E, Krztoń H (2019) Phosphorus recovery from acidic wastewater by hydroxyapatite precipitation. J Environ Manag 232: 421–427

Comodi P, Liu Y (2000) $CO_3$ substitution in apatite: further insight from new crystal-chemical data of Kasekere (Uganda) apatite. Eur J Mineral 12:965–974

Dickens B, Brown WE (1972) The crystal structure of CaKAsO4. $8H_2O$. Acta Cryst B 28:3056–3065

Drizo A, Comeau Y, Forget C, Chapuis RP (2002) Phosphorus saturation potential: a parameter for estimating the longevity of constructed wetland systems. Environ Sci Technol 36:4642–4648

Feng Y, Yu Y, Qiu L, Zhang J, Gao L (2012) The characteristics and application of grain-slag media in a biological aerated filter (BAF). J Ind Eng Chem 18:1051–1057

Forbes MG, Dickson KR, Golden TD, Hudak P, Doyle RD (2004) Dissolved phosphorus retention of light-weight expanded shale and masonry sand used in subsurface flow treatment wetlands. Environ Sci Technol 38:892–898

Gan F, Zhou J, Wang H, Du C, Chen X (2009) Removal of phosphate from aqueous solution by thermally treated natural palygorskite. Water Res 43:2907–2915

Gao Y, Liang B, Chen H, Yin P (2018) An experimental study on the recovery of potassium (K) and phosphorous (P) from synthetic urine by crystallization of magnesium potassium phosphate. Chem Eng J 337:19–29

Gimsing AL, Szilas C, Borggaard OK (2007) Sorption of glyphosate and phosphate by variable-charge tropical soils from Tanzania. Geoderma 138:127–132

Headley TR, Huett DO, Davison L (2003) Seasonal variation in phosphorus removal processes within reed beds–mass balance investigations. Water Sci Technol 48:59–66

Johansson L, Gustafsson JP (2000) Phosphate removal using blast furnace slags and opoka-mechanisms. Water Res 34:259–265

Liang Z, Peng X, Luan Z (2012) Reduction of phosphorus release from high phosphorus soil by red mud. Environ Earth Sci 65:581–588

Liu J, Wan L, Zhang L, Zhou Q (2011) Effect of pH, ionic strength, and temperature on the phosphate adsorption onto lanthanum-doped activated carbon fiber. J Colloid Interface Sci 364:490–496

Luck JD, Workman SR, Coyne MS, Higgins SF (2009) Consequences of manure filtration through pervious concrete during simulated rainfall events. Biosyst Eng 102:417–423

Mitsionis A, Vaimakis T, Trapalis C (2010) The effect of citric acid on the sintering of calcium phosphate bioceramics. Ceram Int 36:623–634

Moulder JF, Stickle WF, Sobol PE, Bomben KD (1992) Handbook of X-ray photoelectron spectroscopy. Perkin-Elmer Corporation Physical Electronics Division, USA

Park JH, Kim SH, Delaune RD, Kang BH, Kang SW, Cho JS, Ok YS, Seo DC (2016) Enhancement of phosphorus removal with near-neutral pH utilizing steel and ferronickel slags for application of constructed wetlands. Ecol Eng 95:612–621

Park JY, Byun HJ, Choi WH, Kang WH (2008) Cement paste column for simultaneous removal of fluoride, phosphate, and nitrate in acidic wastewater. Chemosphere 70:1429–1437

Peng L, Dai H, Wu Y, Peng Y, Lu X (2018) A comprehensive review of phosphorus recovery from wastewater by crystallization processes. Chemosphere 197:768–781

SEPA (State Environmental Protection Administration of China) (2002) Monitor and analysis method of water and wastewater. Chinese Environmental Science Press, Beijing

Shin EW, Han JS, Jang M, Min SH, Park JK, Rowell RM (2004) Phosphate adsorption on aluminum-impregnated mesoporous silicates: surface structure and behavior of adsorbents. Environ Sci Technol 38:912–917

Sleiman N, Deluchat V, Wazne M, Mallet M, Courtin-Nomade A, Kazpard V, Baudu M (2016) Phosphate removal from aqueous solution using ZVI/sand bed reactor: behavior and mechanism. Water Res 99:56–65

Stumm WS and Morgan JJ (1981) Aquatic chemistry: an introduction emphasizing chemical equilibria in natural water. M. 2nd. John Wiley & Sons, Inc. 210, 421, 201

Stumbea D (2013) Preliminaries on pollution risk factors related to mining and ore processing in the Cu-rich pollymetallic belt of EasternCarpathians omania. Environ Sci Pollut Res 20:7643–7655

Wang X, Chen J, KongY SX (2014) Sequestration of phosphorus from wastewater by cement-based or alternative cementitious materials. Water Res 62:88–96

Wang Z, Chen L (2015) Adsorption characteristics of dibutyl phthalate from aqueous solution using ginkgo leaves-activated carbon by chemical activation with zinc chloride. Desalin Water Treat 54: 1969–1980

Wang Z, Zhong M, Chen L (2016) Coal-based granular activated carbon loaded with $MnO_2$ as an efficient adsorbent for removing formaldehyde from aqueous solution. Desalin Water Treat 57:13225–13235

Wang Z, Wang Z, Xu K, Chen L, Lin Z, Liu Y (2019) Performance evaluation of adsorptive removal of Ni(II) by treated waste granular-activated carbon and new granular-activated carbon. Desalin Water Treat 161:315–326

Wilsenach JA, Schuurbiers CA, van Loosdrecht MC (2007) Phosphate and potassium recovery from source separated urine through struvite precipitation. Water Res 41:458–466

Xu K, Wang C, Wang X, Qian Y (2012) Laboratory experiments on simultaneous removal of K and P from synthetic and real urine for nutrient recycle by crystallization of magnesium-potassium-phosphate-hexahydrate in a draft tube and baffle reactor. Chemosphere 88:219–223

Xu N, Li Y, Zheng L, Gao Y, Yin H, Zhao J, Che Z, Chen J, Chen M (2014) Synthesis and application of magnesium amorphous calcium carbonate for removal of high concentration of phosphate. Chem Eng J 251:102–110

Yang S, Zhao Y, Chen R, Feng C, Zhang Z, Lei Z, Yang Y (2013) A novel tablet porous material developed as adsorbent for phosphate removal and recycling. J Colloid Interface Sci 396:197–204

Yang S, Jin P, Wang X, Zhang Q, Chen X (2016) Phosphate recovery through adsorption assisted precipitation using novel precipitation material developed from building waste: behavior and mechanism. Chem Eng J 292:246–254

Yin H, Kong M (2014) Simultaneous removal of ammonium and phosphate from eutrophic waters using natural calcium-rich attapulgite-based versatile adsorbent. Desalination 351:128–137

Yokota R, Hayashi H, Hirata I, Miake Y, Yanagisawa T, Okazaki M (2006) Detailed consideration of physicochemical properties of $CO_3$ apatites as biomaterials in relation to carbonate content using ICP, X-ray diffraction, FT-IR, SEM, and HR-TEM. Dent Mater J 25: 597–603

Yoshimura M, Sujaridworakun P, Koh F, Fujiwara T, Pongkao D, Ahniyaz A (2004) Hydrothermal conversion of calcite crystals to hydroxyapatite. Mater Sci EngC 24:521–525

Yue Q, Zhao Y, Li Q, Li W, Gao B, Han S, Qi Y, Yu H (2010) Research on the characteristics of red mud granular adsorbents (RMGA) for phosphate removal. J Hazard Mater 176:741–748

Zhou AJ (2017) Experimental study on the performance of waste concrete in production of ordinary mortar. N Bull Chin Ceram Soc 36: 620–624